NATIONAL AERONAUTICS AND SPACE ADMINISTRATION

Technical Report 32-1354

A High-Rate Telemetry System for the Mariner Mars 1969 Mission

R. C. Tausworthe
M. F. Easterling
A. J. Spear

JET PROPULSION LABORATORY
CALIFORNIA INSTITUTE OF TECHNOLOGY
PASADENA, CALIFORNIA

April 1, 1969

NATIONAL AERONAUTICS AND SPACE ADMINISTRATION

Technical Report 32-1354

A High-Rate Telemetry System for the Mariner Mars 1969 Mission

R. C. Tausworthe
M. F. Easterling
A. J. Spear

JET PROPULSION LABORATORY
CALIFORNIA INSTITUTE OF TECHNOLOGY
PASADENA, CALIFORNIA

April 1, 1969

TECHNICAL REPORT 32-1354

Prepared Under Contract No. NAS 7-100
National Aeronautics and Space Administration

Preface

The work described in this report was performed by the Telecommunications Division of the Jet Propulsion Laboratory.

Contents

Tables

Figures

Contents (contd)

Figures (contd)

Abstract

A multi-mission, deep-space, high-rate telemetry system has been developed for the *Mariner* Mars 1969 mission. Its rationale, analysis, and development into hardware are described, along with its subsequent planned application to an actual spacecraft mission, whose preparation is in progress. The spacecraft system encodes raw binary data into a comma-free, biorthogonal code that antipodally modulates a square-wave subcarrier. In turn, this subcarrier phase-modulates the downlink carrier. Separate signals are not required for subcarrier, word, or symbol sync; all transmitted sideband power is thus available for data transmission. System design and actual data are presented. These data were taken at several levels of system design and functional verification, including some of the spacecraft performance tests.

A High-Rate Telemetry System for the *Mariner* Mars 1969 Mission

I. Introduction

The JPL high-rate telemetry (HRT) system was developed as an advanced engineering project having three main objectives:

(1) To support specifically the *Mariner* Mars 1969 project by designing, building, verifying, integrating, and operating equipment that will receive data from the *Mariner* spacecraft at a rate of 16,200 bits/s.

(2) To develop prototype HRT ground equipment for the Deep Space Network having multiple-mission capability.

(3) To advance the technology of deep-space communications.

The first objective includes flight- and ground-system verification testing, both on the spacecraft compatibility-test level and at the launch site. The second objective includes the establishment of ranges for the various parameters that may be encountered in future missions (e.g., data rates and subcarrier frequencies), and the design of equipment to handle these ranges. The third objective includes working out all the techniques for system analysis and verification testing required to support the first two objectives.

The first part of the objective required a 25-dB increase in capability over previous deep-space systems. Most of this increase was met with the more straightforward state-of-the-art advances in antenna size, system temperature, and transmitter power; the remaining few decibels were achieved by improved signal-handling techniques.

Briefly, the spacecraft portion of the system encodes raw binary data into a comma-free, biorthogonal code, which then antipodally modulates a square-wave subcarrier. The subcarrier, in turn, phase-modulates the downlink carrier. No separate signal is required for subcarrier, word, or symbol sync; all transmitted sideband power is thus available for data transmission.

The ground portion of the system consists of the usual antenna–receiver complex, a separate subcarrier demodulator, a digital cross-correlator/symbol-timing assembly to effect a maximum-likelihood detection of the received stream, and a general-purpose digital computer to process and record the detected data.

One major achievement of the project, ancillary to the telemetry function provided, was designing and building a system and verifying performance within a very few tenths of a decibel of the theoretical model. An outgrowth of this achievement is that, in the future, a design

engineer need not be concerned so much with assigning *experimental losses* to components, but instead, with considerations of theoretic component *efficiency*.

A. Requirements and History

One major objective of the *Mariner* Mars 1969 two-spacecraft mission is to obtain TV pictures of Mars. These are to be stored onboard at high speed on an analog tape recorder, played back at a lower speed through an analog-to-digital converter (A/DC), and re-recorded on a digital tape recorder. A playback of the digitized tape at a still lower speed will then produce a data stream at a rate that can be transmitted to earth over a more conventional telemetry channel (270 bits/s). It was recognized that the use of two tape recorders in tandem reflected a potentially unreliable situation. A question was raised as to the feasibility of using a special channel that would transmit the data at the playback rate of the analog tape recorder to eliminate one of the tape recorders. Specifically, at 16,200 bits/s, the analog tape recorder in the spacecraft could play back all of the recorded data in slightly less than 3 h.

A study showed that such a high-rate channel could be implemented by using the Goldstone 210-ft diameter antenna if certain operational constraints were accepted. These constraints, the principal one being that the ground antenna operate above a certain minimum elevation angle, proved to be acceptable. As part of the system feasibility study, it was necessary to investigate a number of factors. Starting with the design control table that had already been developed for the *Mariner* Mars 1969 Telecommunications System, the factors that could be changed to increase the capability by the requisite amount were determined.

B. Communications Parameters

The results are summarized in Table 1, which is a simplified version of the design control table for the 16,200-bits/s channel, with the 8⅓-bits/s channel from *Mariner IV* included to extend the comparison. The quantities in Table 1 are related by the standard communication equation,

$$S = P_T M G_T L_S G_R L_R$$

in which P_T is the power produced by the transmitter; M is the modulation loss (i.e., the factor that relates the power in the sidebands to the total power); G_T is the transmitting antenna gain over an isotropic one, including both circuit and pointing losses, as well as antenna gain; L_S is the space loss $\lambda^2/(4\pi)^2 r^2$, in which λ is the wavelength and r is the range; G_R is the receiving antenna gain; L_R is the receiver loss; and S is the received sideband power.

The received sideband power multiplied by the duration of a bit T_B gives the received signal energy per

Table 1. Design control table for *Mariner IV* and *Mariner* Mars 1969

Parameter	*Mariner IV* 8⅓-bits/s channel		Δ, db	*Mariner* Mars 1969 16,200-bits/s channel	
P_T	8.9 W	+39.5 dBmW	+3.10	18.2 W	+42.60 dBmW
M		−5.3 dB	+3.96		−1.34 dB
G_T		+20.1 dB	+0.10		+20.21 dB
L_S	216×10^6 km	−266.2 dB	+6.84	97×10^6 km	−259.36 dB
G_R	85 ft	+52.5 dB	+8.50	210 ft	+61.00 db
L_R		−3.4 dB	+2.96		−0.44 dB
S		−162.8 dBmW	+25.47		−137.33 dBmW
T_B	8⅓ bits/s	−9.2 dB-s	−32.90	16,000 bits/s	−42.10 dB-s
ST_B		−172.0 dBm-s	−7.43		−179.43 dBmW-s
N_0	65°K	−180.5 dBmW/Hz	+4.10	25°K	−184.60 dBmW/Hz
ST_B/N_0		+8.5 dB	−3.33		+5.17 dB
Required ST_B/N_0	5×10^{-3} BER[a]	+5.20 dB	+2.20	1×10^{-2} WER[b]	+3.00 dB
Margin		+3.3 dB	−1.13		+2.17 dB

[a]BER = bit error rate.
[b]WER = word error rate.

bit. The receiver system effective noise temperature multiplied by Boltzmann's constant gives the receiver noise spectral density. Together, these specify the appropriate figure of merit ST_B/N_0 for a digital communication system. Dividing the achieved figure of merit by that required for a specified performance gives the margin. The Δ column in Table 1 shows the change from one system to the next, considered positive if it favors the second system.

The increase in capability from 8⅓ bits/s for *Mariner IV* to 16,200 bits/s for the high-rate channel on *Mariner* Mars 1969 is due to many factors.

First, the transmitter power has been approximately doubled since *Mariner IV*. Next, the modulation index was changed to increase the sideband power from −5.3 to −1.80 dB relative to the total power. Two factors made this possible. First, the *Mariner* Mars 1969 telemetry system does not use a separate synchronizing channel; thus, the power that was so used in the earlier system is available for data transmission. Second, the high data-rate-to-carrier-loop-bandwidth ratio makes it feasible to assign much less relative power to the carrier component of the downlink signal to effect synchronous demodulation.

The design control table does not show a significant change in the spacecraft antenna gain, although a larger antenna is used for the *Mariner* Mars 1969 mission. The potentially increased gain was traded for other considerations; e.g., using a single pointing angle for the antennas on both spacecraft, even though they arrive at Mars on different days.

The range at encounter will be about half what it was for *Mariner IV*. This increases the communications capability by 6.84 dB; it is not a change in the communications technology per se.

The 8.50-dB increase in ground antenna gain is slightly more than a mere area increase because of improved tolerances. In the detailed design control table, each parameter is assigned a nominal value, along with a favorable and an unfavorable tolerance. The system design is constrained to provide adequate performance with all of the parameters having their full unfavorable tolerances. This is the usual and accepted philosophy in all engineering work: design proceeds with all elements derated by an appropriate factor. Because there is only one 210-ft antenna, closely and continually maintained, it has a lower unfavorable tolerance than the worst-of-a-network value that must be used in dealing with a set of antennas located around the world.

There are other reasons why the tolerance in this particular case is less. When an antenna is moved from pointing at the zenith to pointing at the horizon, there is sag due to gravity, and the gain changes. In the case of the high-rate channel, the total time required to play back the data from the analog recorder in the spacecraft is less than 3 h, and can be selected to take place when the 210-ft antenna angle is greater than 25 deg. Also, if there were an unusually high wind on the day when playback is desired, it could delay playback for a day.

The effect of these factors gives the 210-ft antenna the higher usable gain. The cost of this gain is a set of restrictions on its operation. Because the playback time is short and selectable, these restrictions are acceptable.

System temperature is also significantly improved due to two factors: (1) because the 210-ft antenna will not be required to transmit during the short time it is receiving the high-rate data, a listen-only feed system of advanced design can be used; and (2) since the minimum elevation angle is 25 deg, the antenna need not look obliquely through the atmosphere. However, the temperature of the receiving system will begin to rise if the rainfall rate exceeds 0.1 in./h, but this is unlikely in the Mojave desert in August.

Entry L_R (receiver loss) in Table 1 includes many factors. One factor is the degraded synchronous demodulation effected by carrier-loop jitter; i.e., by detection-reference noise. For example, *Mariner IV* was constrained to a relatively low signal-to-noise ratio (SNR) in the carrier tracking loop; although the power allocation was optimized, the effect was equivalent to a loss of more than 2 dB. In the *Mariner* Mars 1969 high-rate channel, however (even though the power allocation is reoptimized with proportionately less power in the carrier), the carrier has more absolute power, and the effect of data degradation caused by noise in the carrier loop is less than 0.1 dB in equivalent signal power.

A second factor is the SNR in the bandwidth of the subcarrier tracking loop. Again, in the case of *Mariner IV*, this loop was constrained to have a rather poor SNR. In addition, although a square-wave subcarrier was used, the demodulation process was able to recover only the power carried in the fundamental. The total equivalent loss was greater than 1 dB. In the *Mariner* Mars 1969

system, the different method of tracking the subcarrier uses the entire sideband power, with its inherently higher SNR. Furthermore, the demodulation technique recovers all power in the data, up to the fifth harmonic. The combined result is a much smaller equivalent signal loss. Finally, there are small losses associated with symbol tracking, data detection, and circuit imperfections. In summary, the higher ratio of data rate to carrier-loop bandwidth permits a reduction in effective loss caused by a noisy carrier reference. Improved methods of subcarrier and symbol tracking and of data detection permit the recovery of a greater portion of the sideband power.

The final factor to be considered is the ST_B/N_0 required to transmit data with an error rate not exceeding 5×10^{-3}. If bit-by-bit detection were used, as in previous *Mariners,* the required ST_B/N_0 would be 5.20 dB after all losses (or equivalent losses) are considered. If the data are encoded 6 bits at a time into a biorthogonal code, however, the required ST_B/N_0 is reduced to only 3.00 dB for a word-error rate of 10^{-2} (equivalent to a bit-error rate of 5×10^{-3}). Thus, with all other factors equal, block coding reduces the required signal level by 2.20 dB.

The margin shown in Table 1 represents performance at encounter, and must be large enough to maintain a positive margin over the entire playback period. Since the high-rate channel recovers the data in less than 3 h, only a small margin is needed even if it is necessary to play back the data on several successive days.

The purpose of the preceding discussion has been to show the rationale indicating that a high-rate channel for *Mariner* Mars 1969 is feasible, to enumerate several important factors, and to define the operational constraints under which the channel could be used. Numbers in Table 1 have been subjected to continuous refinement; hence, the values given, although typical, must be considered as only illustrative of the type of performance that can be expected. The total situation is somewhat more complex than that indicated because a low data-rate channel, on a separate subcarrier, is also present whenever the high-rate channel is being used. The presence of this second channel reduces the performance margin slightly. Although its effect is only incidentally referred to here, the detail design considers it. The conclusions that have been drawn, however, remain unchanged.

C. Equipment and Schedule

Because the primary objective of the HRT project is to support the *Mariner* Mars 1969 project, certain equipment had to be produced on a time scale consistent with the flight schedule. Although the operation date is not until after encounter in mid-1969, equipment was needed as early as January 1968 to assist in the testing of the spacecraft proof-test model. The high-rate system is experimental in that it involves both new equipment and, to some extent, new techniques in the area of subcarrier tracking and data synchronization. It was considered desirable, therefore, to engineer a prototype before constructing the actual field sets. Since time was very short, the initial spacecraft testing would proceed with the prototype system. Figure 1, a simplified version of the project schedule, shows the important milestones and periods of required support.

It was recognized early that special techniques for testing the system would have to be devised. Therefore, the team constructed a slow-speed laboratory version of the system, and began to run various tests during the time that the prototype system was under development.

The prototype system (Lab Set A) was designed, tested, and had its performance completely verified by the end of January 1968. At that time, it was installed in the Flight Project/Tracking and Data Acquisition Interface Laboratory (CTA-21) to support the spacecraft proof-test model until the actual field sets could be completed.

In mid-1968, the actual flight spacecraft were scheduled for delivery. To provide for that support, the first of two field sets was installed. The field sets are functionally the same as Lab Set A, but advantage was taken of the interim experience to produce more fieldworthy equipment.

In November 1968, the prelaunch operations at Cape Kennedy began. To support this activity, the first field set was installed there. To maintain continuous capability in CTA-21, the second field set was installed there, and it was fully qualified.

After launch, both field sets will be moved to the Goldstone 210-ft antenna site (DSS 14) to support the operation at encounter. Two field sets are provided for a complete redundant ground system.

After Lab Set A was removed from CTA-21, it was used in additional laboratory tests to further refine techniques. When both field sets are sent to DSS 14, Lab Set A will be reinstalled in CTA-21 to provide a complete capability for mating with the proof-test model spacecraft should questions arise regarding the designed response of the flight spacecraft during the flight.

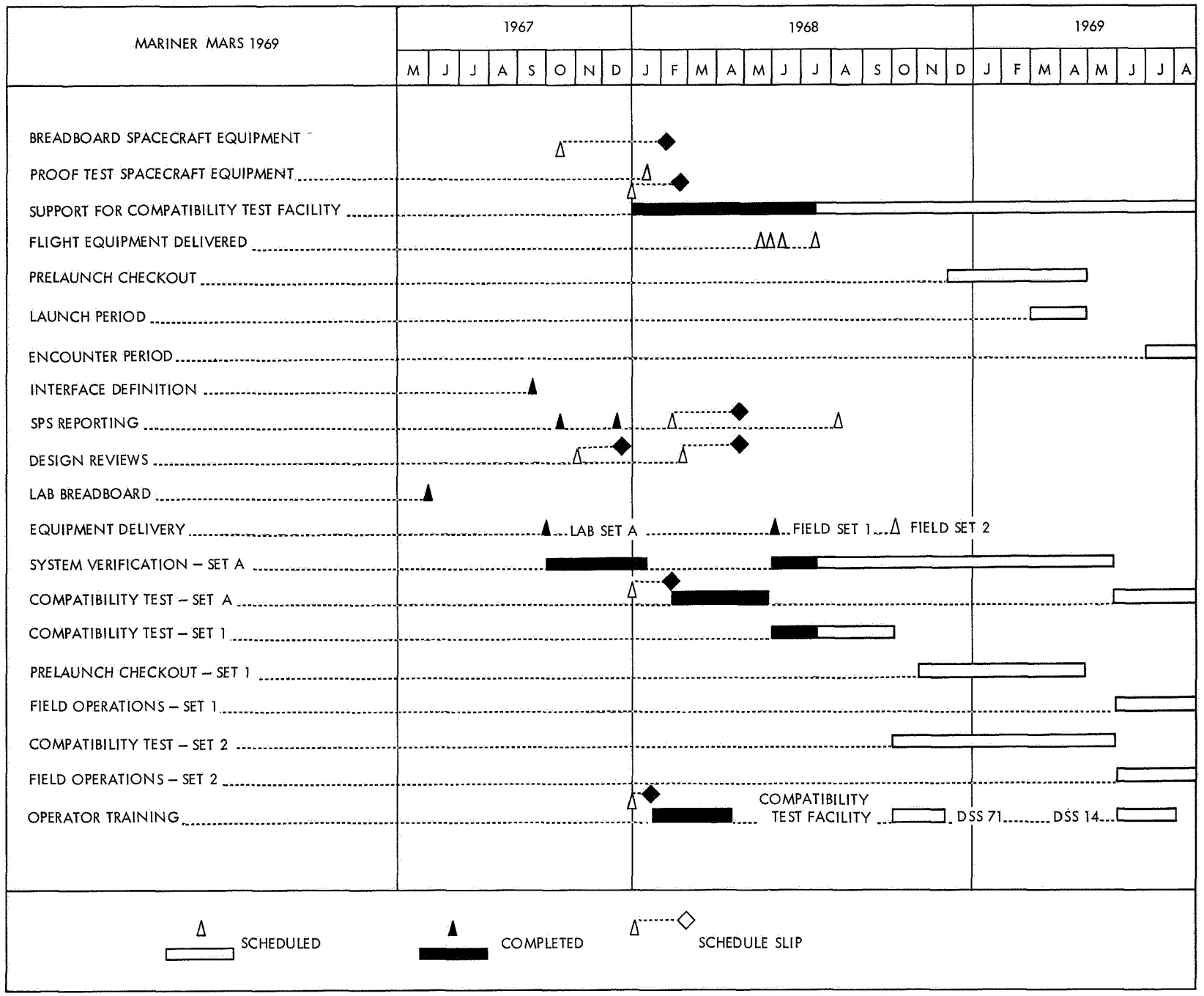

Fig. 1. Abstract of HRT project schedule

II. System Functional Design

The HRT system embodies techniques and theories that have been developed at JPL and instituted as a direct result of the consideration noted above. It is a modification of the basic digital telemetry system that was used on both *Mariners IV* and *V*. The HRT system differs, however, in that the data are block-coded, there is no sync channel, and the detection process is more efficient.

A. Functional Design

A block diagram showing the functional organization of the HRT system is shown in Fig. 2. Data are block-encoded 6 bits at a time into words of 32 binary symbols, then biphase-modulated onto a square-wave subcarrier. The modulated subcarrier, in turn, phase-modulates the downlink carrier for transmission. On the ground, the Deep Space Instrumentation Facility (DSIF) receiver tracks the carrier and provides a reference for synchronously demodulating it. The subcarrier loop tracks the subcarrier and provides a reference for synchronously demodulating the subcarrier. The symbol loop tracks the symbol transitions and provides timing to the cross-correlation detector. The output of the detector is the recovered bit stream, which is then recorded for the data user. In the actual hardware, the functions are slightly rearranged; in some cases, they are combined to simplify the equipment, but the functions performed are the same.

B. Signal Structure and its Rationale

In the preceding discussion, allusions have been made to square-wave subcarriers, multiple channels, and coherent carrier detection without, as yet, a clear definition of the nature of the composite downlink waveform or the reasons why it is that way. The signalling aspect of the telemetry function is presented below, concerning not so much the equipment involved, but the types of channels, rates, allotted bandwidths, power allocation, and signal waveform optimization for which provision is made.

The first restriction on the waveform is one placed on the system, not by the telemetry function, but by a flight-project requirement for coherent two-way doppler extraction. In the present implementation of the DSIF, this can only be achieved by leaving an unmodulated carrier component of sufficient strength for the receiver to acquire and phase-track reliably. In order not to degrade data quality or hamper carrier acquisition, information is modulated onto subcarriers to move them well outside the tracking bandwidth of the receiver. The choice of biphase modulation of square-wave subcarriers is due to the fact that there is potentially very little loss in the modulation sidebands, either as unrecoverable harmonics or as cross-modulation products. This is obvious in the trigonometric expansion of expressions of the form, A sin $[\omega_0 t + \theta_0 + \theta_1(t) + \theta_2(t)]$, in which $\theta_1(t)$ represents binary angle modulations. The unrecovered power (i.e.,

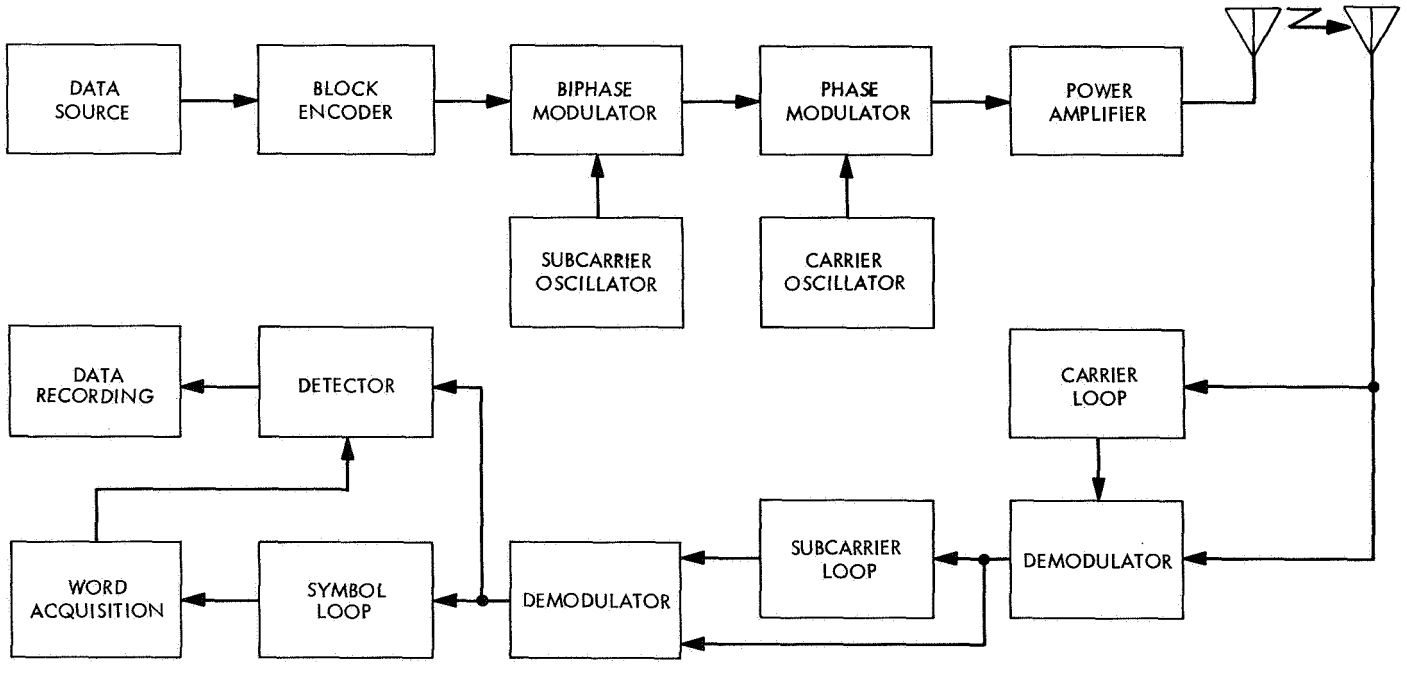

Fig. 2. High-rate telemetry system functional diagram

power not recoverable by simple matched filtering) is $P_{loss} = P_1P_2/P_{carr}$, where P_1 and P_2 are the respective powers given to each of the square-wave subchannels. The ratio P_{loss}/P_{total} is relatively minor when one of the channels is given a low modulation index, as is normally the case when there are wide differences in the data rates of the two channels. A further advantage of binary modulation is that the output process spectral density does not change in form as a function of the modulation index.

In the *Mariner* Mars 1969 as the case in point, there are three separate channels, but no more than two are ever actuated at one time. During the cruise phase of the mission, only engineering data are transmitted, at a rate selectable as either 33⅓ or 8⅓ bits/s. Then, at such time as science data are to be transmitted (e.g., at encounter, or as a subsequent playback), the normal science channel can be activated at a data rate selectable as either 66⅔ or 270 bits/s. An alternate science-data transmission mode, however, is the much higher rate of 16,200 bits/s, which is, of course, the mode that is of concern here. The large disparity between the engineering and science data rates means that relatively little power need be allocated to the engineering data to achieve comparable bit-error rates in the two channels. In addition, the removal of the necessity for a separate bit/word-sync channel by the subcarrier demodulation technique that is used not only allows greater power to be allocated to the data, but also prevents the losses that a third channel would cause.

Bandwidth allocation for *Mariner* Mars 1969 telemetry is approximately 3 MHz about the carrier, or about 1.5 MHz at the modulator input terminals. A design goal of 0.1 dB degradation due to spectral filtering was sought. Calculations showed that this could be achieved only if energy up to at least the fifth harmonic were retained in the transmitted signal. However, transmitting 16,200 bits/s biorthogonally encoded over a channel with such a bandwidth constraint limits both the degree of encoding (i.e., the average number of symbols/bit) and the subcarrier frequency to relatively low figures. A (32,6) code with three subcarrier cycles/symbol would fit in the band, and marginally, the (64,7) with two subcarrier cycles/symbol. The latter might theoretically result in about a 0.2-dB SNR advantage over the former, but it would require a cross-correlator with twice the complexity. Hence, the (32,6) code was chosen as one near the point of diminishing returns that would demonstrate the advantages of block coding, and would not be too costly to implement. In considerations of the logic speed required to combine data and subcarrier, it was necessary to make the subcarrier waveform coherent with the symbol transitions.

III. Performance Calculations

As a general rule, early in the development of a high-performance system, the designer calculates its expected performance based on a set of assumed and desired parameters. From these, specifications are then derived to guide the various specialists in developing the hardware and software that compose the overall system. Because these specialists may have an imperfect understanding of the total system, and because the system designer himself may not be fully versed in the technology of each part, there can be a potential problem in translating the system parameters into subsystem specifications. This problem can be greatly alleviated, however, if the performance calculations are based on system parameters that are directly interpretable as subsystem specifications. The remainder of this section presents an efficiency concept that seems particularly well suited, not only to the HRT system, but to any system in which the several parts are connected in tandem.

A. Parameters for the Spacecraft Subsystem

If all of the parts of the transmitter (shown in the spacecraft system in Fig. 2) functioned perfectly, the transmitter would have no deleterious effect on system performance. This is in contrast to the receiver, which, even when functioning perfectly, degrades performance because of thermal noise. Because of spacecraft weight and power limitations, there is a need to allow some imperfection in the transmitter and to relate that imperfection to system performance. Another factor that must be considered in specifying the transmitter is its natural interface at the input to the phase modulator. The equipment up to this point is essentially digital; following this point, it is essentially analog (i.e., RF). The two parts are likely to be assigned to different development teams; in the *Mariner* Mars 1969 system, for example, they went to two different contractors. All things considered, it is thus almost mandatory to specify the transmitter characteristics in terms of a set of quantities reflecting the various design aspects of that subsystem; e.g., (1) modulation waveform, (2) modulation index, and (3) RF spectrum.

The modulation waveform specification, as a case in point, should allow for a certain degree of imperfection, as illustrated in Fig. 3, which shows one subcarrier cycle at the input to the phase modulator. Figure 3 also shows an ideal waveform that has the same period as the actual waveform and the same amplitude as the flattest portion of the actual waveform. The cross-correlation of the actual and ideal waveforms gives the amplitude of the equivalent recoverable ideal waveform. The power in the ideal waveform is $P_I = A^2$, whereas the power in the recoverable

portion of the actual waveform is $P_A = (\rho A)^2$, where ρ is the normalized cross-correlation. The fractional loss in power then is

$$\text{loss} = \frac{A^2 - (\rho A)^2}{A^2}$$

$$= 1 - \rho^2$$

and the power efficiency is ρ^2.

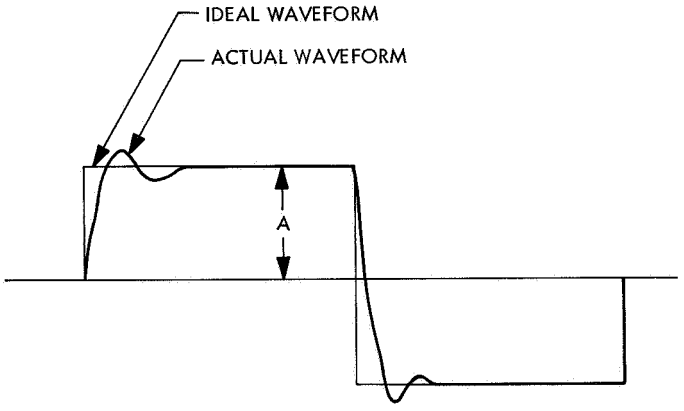

Fig. 3. One cycle of subcarrier waveform, actual and ideal

The required efficiency is set by the system designer, and is used as a design specification by the equipment designer. Efficiency is a common language for both, and is more suitable than such factors as rise time, over-shoot, and asymmetry because it gives the equipment designer the option of taking the permitted loss in the most advantageous way, rather than in some arbitrarily imposed way. Because any imperfection is a loss compared to the ideal model, the various parts of the system can be designed and tested separately with the assurance that, once connected, the overall performance will be at least as good as predicted. In a high-performance system, this implies that the overall performance will be in a narrow region slightly better than predicted performance.

The modulation index (the second item above) can be specified by the system designer in terms of carrier suppression; i.e., if a perfect square wave of a certain amplitude is applied to the modulator input, the unmodulated component at the output of the transmitter will be reduced by a certain proportion. The assignment of this index is based on the desired allocation of power between the carrier and the sidebands. The designer assumes that all power not in the carrier is in sidebands (a good assumption because the transmitter power amplifier is saturated), and that all of the sideband power is available for telemetry. Tolerances are assigned to the modulation index and to the amplitude of the subcarrier; deviations of either from the desired value and cross-channel products (where present) are treated as a loss of efficiency in producing either carrier or sideband power, as appropriate. In *Mariner* Mars 1969, the overall system performance is extremely sensitive to sideband power loss; therefore, the specifications including tolerances were established accordingly.

Some comments on system and subsystem testing are in order before proceeding with the discussion of analysis techniques. Equipment specifications are useful only if the equipment can be tested to verify those specifications. This is the primary reason for the modulation index to be specified in terms of carrier suppression, rather than modulation angle, which is a quantity more convenient for the system designer. Commonly available RF-measurement techniques permit suppression ratios to be determined with great precision. Furthermore, it is possible, by using laboratory test equipment, to generate test square waves with very precisely controlled waveforms and amplitudes, permitting the modulation index, from the modulation input to the power amplifier output, to be measured very accurately. A similar comment can be made concerning the measurement of the output amplitude of the digital equipment in comparison with a waveform produced by laboratory equipment.

The RF spectrum at the power amplifier output can be specified in terms of the ideal spectrum that would normally be produced by a perfect squarewave at the subcarrier frequency. It is easy to compute the relative power in the several sidebands and to measure that power when a test square wave modulates the transmitter. Any deviation of the power in any sideband from the desired power can be interpreted as a loss, and the sum of these power losses is the quantity specified. This is equivalent to specifying the efficiency of the RF portion of the transmitter in converting the modulating waveform to desired sidebands. (The effect of imperfections in the modulating waveform has already been taken into account.) The overall efficiency of the transmitter is given by the product of the efficiencies of the modulating waveform, the modulation index, and the RF spectrum.

B. Analysis of the Receiver

As shown in the system block diagram (see Fig. 2), there are three loops, each followed by a demodulation or detection process. In each case, the process is performed imperfectly for two reasons: (1) noise causes the output

of the loop to jitter in phase or time, and (2) imperfections in the equipment or software either cause the waveforms into the process to be distorted or displaced or cause the process to be imperfectly carried out. Each of these results in a reduction in the available signal power at the output of the process, but has little effect on the noise power at the output of the process. Unlike transmitter efficiency, which is expressible in terms of available power relative to potentially available power, the receiver efficiency is properly expressed in terms of available SNR relative to potentially available SNR. The effect of each of the loops and its associated process can be expressed as

$$\left(\frac{ST_B}{N_0}\right)_{out} = \eta\delta \left(\frac{ST_B}{N_0}\right)_{in}$$

where η is the theoretical efficiency due to the effect of the SNR in the loop, and δ is the efficiency due to the imperfections. Because the former efficiencies themselves are functions of the SNR, the values to be used in the design specification are those that apply at the minimum SNR for which the receiver is supposed to deliver the specified performance (i.e., bit-error rate). This is the minimum operating condition of the device.

The processes for which these efficiencies can be defined and computed in the most straightforward manner are those for the subcarrier loop and subcarrier demodulator. This equipment is primarily analog and has three different selectable bandwidths. The theoretical efficiency for any bandwidth setting and for a given bit-error rate is a function of the information rate. This is true because the required signal/noise-spectral-density ratio varies as a function of the information rate. The form of this efficiency curve (Ref. 1), which is shown in Fig. 4, is expressed as equivalent signal loss for increased precision. Both the theoretical efficiency and the combined efficiency are specified to the equipment designer, along with the loop bandwidths to be used. The efficiency curves, then, are a common language for the equipment designer and the system designer.

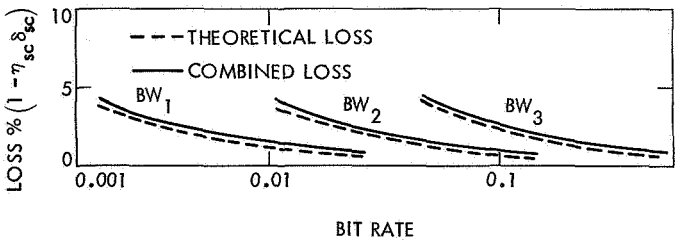

Fig. 4. Subcarrier-loop efficiency

The symbol loop is slightly less straightforward because it is more meaningful to separate the efficiency of symbol tracking from that of the detection process. The appropriate efficiency for the symbol-tracking loop is the ratio of SNR required for a given error rate when the detector is provided with perfect timing to the SNR required when the symbol loop provides the timing. Again, there are two parts to the efficiency, the one associated with theoretical degradation due the loop, the other with equipment imperfections. In the HRT system, the symbol-loop tracking filter is implemented in a computer, and any bandwidth can be selected to average over a specified number of bits. The form of the efficiency curve (Ref. 2) is shown in Fig. 5, again as a loss in order to enhance the accuracy.

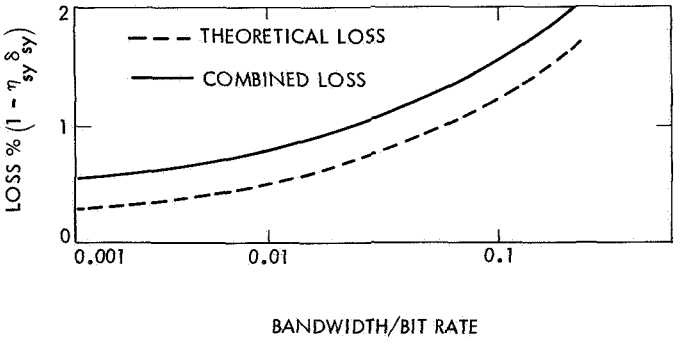

Fig. 5. Symbol-loop efficiency

The carrier loop has the same sort of efficiencies, but the situation is complicated by the fact that the loop bandwidth cannot be selected arbitrarily, and by the additional fact that the loop noise is determined by the carrier SNR rather than the sideband SNR. A detailed description of the optimization process (Ref. 3) by which power is allocated between the carrier and sidebands for best communication performance is outside the scope of this report. However, once the power allocation has been made and one of the permissible bandwidths (i.e., one already existing in the tracking station receiving system) has been selected, there are an appropriate η and δ for the carrier-tracking loop. This varies somewhat with bit rate, but at rates greater than a few thousand bits/second and at the narrowest available loop bandwidth (12 Hz), the efficiencies are high and essentially independent of the bit rate.

Finally, there are considerations of the detector itself. Of course, it is not quite perfect, even though it is a digital device, so there is a δ associated with it for a given probability of error, i.e.,

$$\left(\frac{ST_B}{N_0}\right)_{theor} = \delta_d \left(\frac{ST_B}{N_0}\right)_{actual}$$

In the past, some question has been raised about the proper way to assign a theoretical efficiency. There is, however, a theoretical, absolute standard for comparison that represents the best possible performance, independent of bit-error rate; namely, the Shannon limit. With this choice, the theoretical efficiency can be defined, for a particular design-error rate, as the ratio

$$\eta_d = \frac{\ln 2}{\left(\frac{ST_B}{N_0}\right)_{\text{theor}}}$$

In this way, the theoretical efficiency is a measure of the quality of the signalling/detection process, and the δ efficiency is a measure of how well the process is carried out. This is somewhat analogous to the approach used in thermodynamics wherein the cycle chosen is compared to the Carnot cycle to determine its theoretical cycle efficiency, as distinguished from the implemented efficiency of the machinery in carrying out its assigned task.

C. System Efficiency

The performance of the system can now be computed or specified in several different ways. In terms of subscripts *C*, *SC*, *SY*, and *d*, which refer to the carrier loop, the subcarrier loop, the symbol-tracking loop, and the detector, respectively, the overall efficiency of the receiver, relative to the best that could be done, is

$$\text{Overall Receiver Efficiency} = \eta_C\, \delta_C\, \eta_{SC}\, \delta_{SC}\, \eta_{SY}\, \delta_{SY}\, \eta_d\, \delta_d$$

Similarly, the receiver efficiency, relative to the best that can ever be done using the same signalling/detection scheme, is

$$\text{Relative Receiver Efficiency} = \eta_C\, \delta_C\, \eta_{SC}\, \delta_{SC}\, \eta_{SY}\, \delta_{SY}\, \delta_d$$

Either of these efficiencies can be multiplied by the spacecraft efficiency to obtain a total system efficiency—in the first case, absolute; in the second case, relative. The absolute efficiency is useful in comparing the performance of a particular system with other systems at the same error rate. The relative efficiency is useful in assigning specifications to the various parts of a system under development and in verifying the performance of the completed system. Both approaches have been used in the development of the HRT system, and each has proved to be useful.

IV. System Description

At this point, the rationale and many of the parameters in the design have been established. It remains now to show some of the specific designs and to go into the equipment descriptions and analyses in a little more detail.

A. Flight Equipment

As indicated earlier, the spacecraft transforms the uncoded science data, 6 bits at a time, into 32 binary symbols, which then antipodally modulate a square-wave subcarrier (Fig. 6). The symbol rate is thus 86,400 symbols/s, and the subcarrier is 259,200 Hz. This waveform, together with a similarly modulated engineering data signal, is frequency-multiplexed onto the S-band carrier.

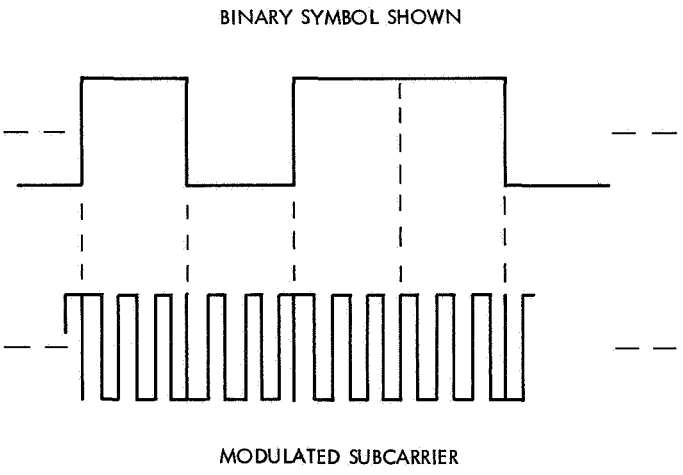

Fig. 6. Symbol and modulated subcarrier waveforms

The spacecraft portion of the high-rate channel is shown in Fig. 7. As indicated, there are two possible sources of data to the encoder. The real-time encounter data source represents some of the data taken as the spacecraft passes near the planet. It is comprised of portions of TV photographs taken of the planet, infrared radiometer data, and infrared and ultraviolet spectrometer data. These data are stored on magnetic tape for playback after encounter; during this recording, however, the high-rate channel may be used for a simultaneous transmission in real time to earth.

The transmitted signal is of the form

$$(2P_T)^{1/2} \cos\left[\omega_c t + \theta_E E(t) + \theta_S S(t)\right]$$

where P_T is the total power, $\theta_E E(t)$ and $\theta_S S(t)$ represent the engineering and science subcarriers modulated with their respective data sequences, θ_E and θ_S, which represent the peak phase deviations of the modulated signal, and $E(t)$ and $S(t)$ are the normalized square-wave signals,

sequencing between the ±1 binary states. Power allocations for carrier, engineering, and science channels are thus given by

$$\frac{P_{carr}}{P_T} = (\cos\theta_E \cos\theta_S)^2$$

$$\frac{P_{sci}}{P_T} = (\cos\theta_E \sin\theta_S)^2$$

$$\frac{P_{eng}}{P_T} = (\sin\theta_E \cos\theta_S)^2$$

The values of θ_E and θ_S are adjusted to meet the individual power requirements for each channel.

The values chosen for the *Mariner* Mars 1969 design are $\theta_E = 12$ deg and $\theta_S = 65$ deg, resulting in power allocations of 17, 80, and 0.8% for the carrier, science, and engineering channels, respectively, in accordance with the data-rate and tracking requirements previously mentioned. A lower value of carrier power would have been permissible, but the stability of the modulation is such that a drift might have suppressed the carrier entirely. The large requirement of the science channel relative to the other channels is because of its large data rate. Even with their respectively lower power allocations, the carrier and engineering power requirements are more than satisfied. Only 2.2% of the power is lost in the cross-modulation products of the two subcarriers.

In keeping with the system efficiency concept discussed in Section III, particular care was given to the preservation of waveforms through the spacecraft telemetry channel. This was especially necessary for the high-rate signal, because its bandwidth occupancy was much greater than was necessary in previous *Mariner* designs. The block-coded channel was made sufficiently wideband and linear to pass the signal spectrum, without significant distortion out to the seventh harmonic of the 259.2-kHz subcarrier. Care was also taken to keep asymmetry in the subcarrier waveform to a minimum.

The heart of the spacecraft HRT system is the block coder. A 32-symbol block-coded word $\mathbf{S}_i$ is generated from a 6-bit data word $\mathbf{D}_i$ in accordance with the matrix operation

$$\mathbf{S}_i = \mathbf{GMD}_i$$

The matrices **G** and **M** are given in Fig. 8. A functional block diagram of the encoder (and implementation of this equation) is shown in Fig. 9. The inputs are the data bits, along with bit and word sync. Six bit-sync and 32 symbol-sync pulses occur for each word-sync pulse. The serial input bit-stream is shifted into a 5-stage register (the input data register) by bit-sync pulses. The contents of this register are added, modulo two, with the high-order bit of the data word input and transferred by the word-sync pulse in parallel into the encoder data register. The high-order bit itself is transferred as it is. The data thus inserted into the encoder data register are the product of the input data vector $\mathbf{D}_i$ multiplied by the matrix **M**.

The rows of the **G** matrix, exclusive of the first element, are generated by a binary counter. The first column of **G** is constant, and thus is automatically taken into account. The code symbols are formed serially by computing the inner product of the contents of the encoder register and

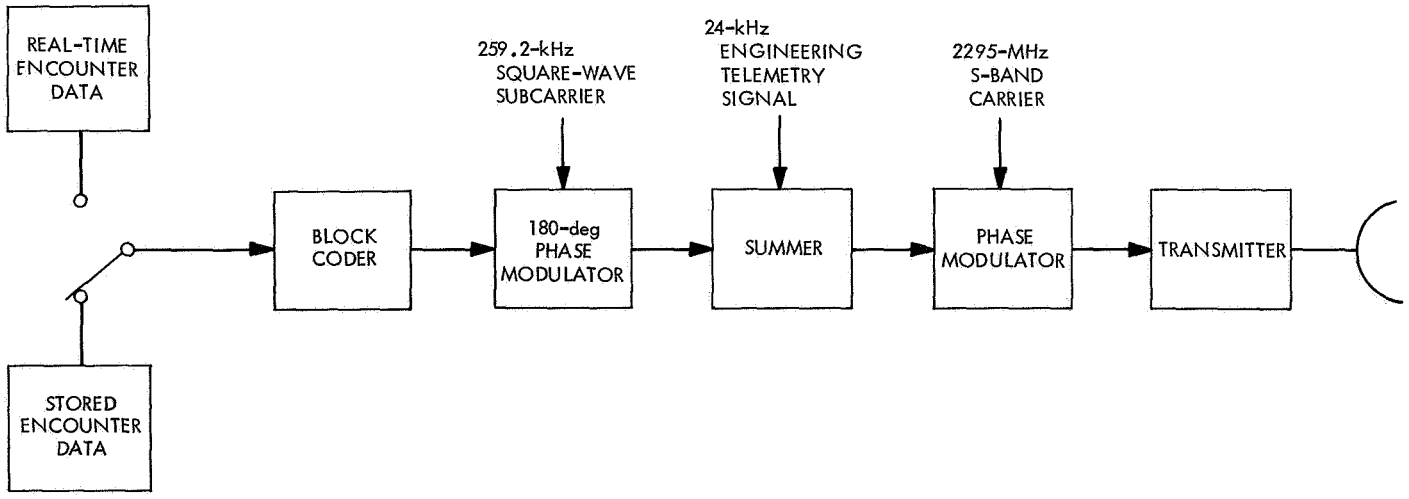

Fig. 7. The spacecraft high-rate telemetry system

that of the binary counter. The result is the Reed–Muller biorthogonal code. Next, the code words are made comma-free so that word sync may be derived on the ground. Comma-freedom in a code means that any 32-symbol string composed of the last 32-N symbols of one code word in juxtaposition with the first N of the next code word (i.e., an overlap of N symbols) is forbidden as a member of the code dictionary. The minimum number of disagreements for all N overlaps of all pairs of words is called the *index* of comma-freedom for that code (Ref. 4).

The Reed–Muller biorthogonal codes are easily made comma-free by adding a particular fixed vector (or word), modulo two, to each of the generated words above. The final coded word $\mathbf{Y}_i$ out of the block encoder is

$$\mathbf{Y}_i = \mathbf{S}_i \oplus \mathbf{C} = (S_{1,i} \oplus C_1, S_{2,i} \oplus C_2, \cdots, S_{32,i} \oplus C_{32})$$

where $\oplus$ denotes modulo two addition, S_{ij} is the *jth* symbol of the *ith* word, and C = (10001101110101000010010110011111) is the comma-free vector. It is an augmented pseudonoise sequence generated in a standard way by a 5-stage shift register. The least significant bit of the incoming data word, as indicated in Table 2, is the first to enter the encoder. Symbol t_0 is the first to leave the encoder.

[G] =

1	0	0	0	0	0
1	0	0	0	0	1
1	0	0	0	1	0
1	0	0	0	1	1
1	0	0	1	0	0
1	0	0	1	0	1
1	0	0	1	1	0
1	0	0	1	1	1
1	0	1	0	0	0
1	0	1	0	0	1
1	0	1	0	1	0
1	0	1	0	1	1
1	0	1	1	0	0
1	0	1	1	0	1
1	0	1	1	1	0
1	0	1	1	1	1
1	1	0	0	0	0
1	1	0	0	0	1
1	1	0	0	1	0
1	1	0	0	1	1
1	1	0	1	0	0
1	1	0	1	0	1
1	1	0	1	1	0
1	1	0	1	1	1
1	1	1	0	0	0
1	1	1	0	0	1
1	1	1	0	1	0
1	1	1	0	1	1
1	1	1	1	0	0
1	1	1	1	0	1
1	1	1	1	1	0
1	1	1	1	1	1

[M] =

1	0	0	0	0	0
1	1	0	0	0	0
1	0	1	0	0	0
1	0	0	1	0	0
1	0	0	0	1	0
1	0	0	0	0	1

Fig. 8. The (32,6) biorthogonal Reed–Muller encoding matrices

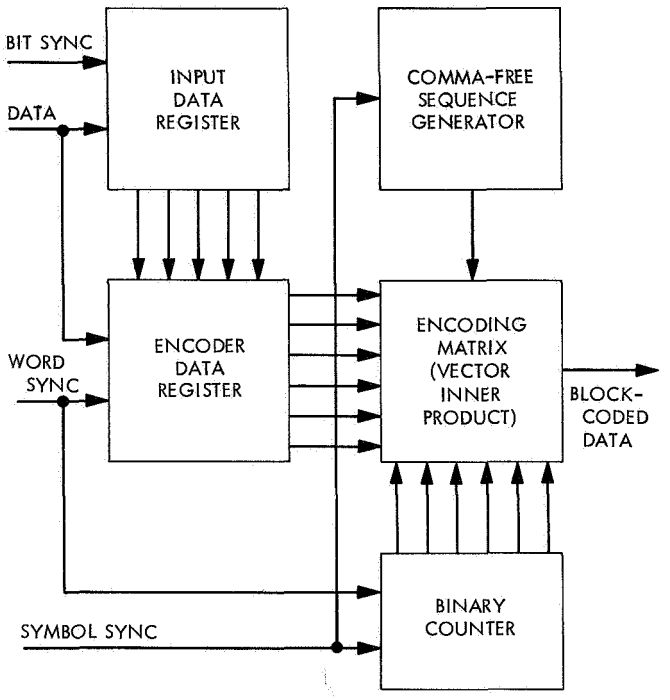

Fig. 9. Encoder block diagram

B. The Ground Telemetry System

The HRT ground equipment being developed is intended to fit into a standard DSIF tracking station. It will connect into the S-band receiver, which will require only a minor modification to accommodate it. This equipment will also use the computer that is part of the telemetry and command data (TCD) subsystem, with no change being made to the computer.

The equipment that performs the functions previously described is divided into three major assemblies. One is the subcarrier demodulator assembly, which contains the subcarrier loop and the data channel down through

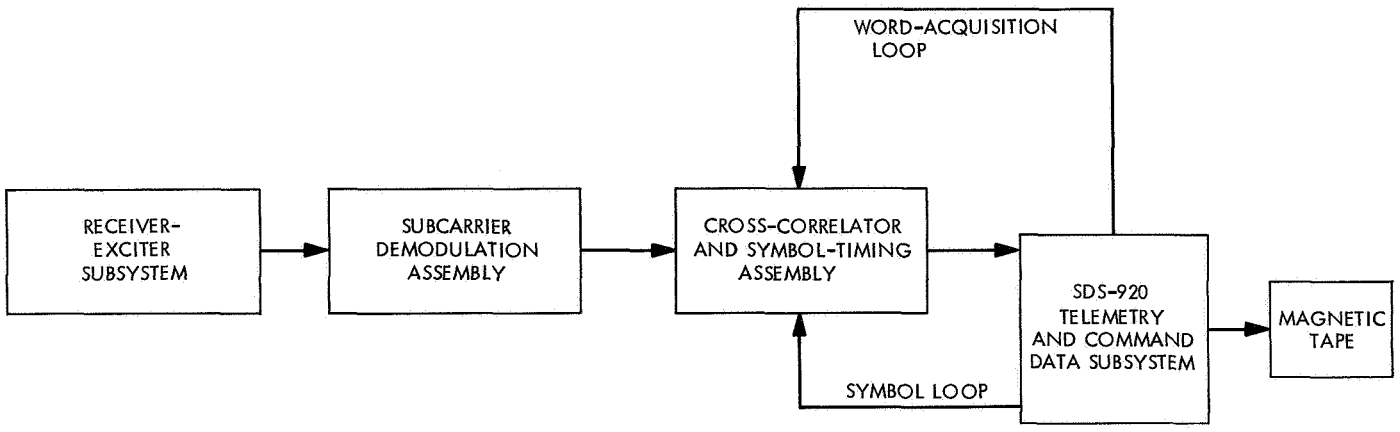

Fig. 10. The HRT ground system

a convenient point for analog-to-digital conversion. This assembly is primarily analog equipment and henceforth will be a part of the receiver subsystem. The second assembly is digital equipment constructed as peripheral equipment for the third assembly, the computer in the TCD subsystem. The computer acts as the overall control device for symbol tracking, data detection, and output recording. A block diagram of the ground portion of the system is shown in Fig. 10. The receiver operates to produce a 10-MHz version of the received signal, fixed both in frequency and in phase. The equipment whose functions are shown in Fig. 10 acts to extract the data from this signal and to record these data digitally on magnetic tape for delivery to the user.

1. Subcarrier demodulator. The first step in the process is the synchronous demodulation of the subcarrier. To facilitate the design of the equipment (Fig. 11), it is convenient to do this before demodulating the carrier. After amplifying and filtering it in the 10-MHz IF amplifier, the data waveform is then recovered by synchronously demodulating the carrier.

The reference that is used to demodulate the subcarrier is provided by a phase-locked loop tracking the subcarrier.

Table 2. Data word/biorthogonal code correspondence

Word No.	Data Word			Coded Word															
				t_0 → Time → t_{3i}															
0	00	00	00	00	00	00	00	00	00	00	00	00	00	00	00	00	00	00	00
1	00	00	01	01	01	01	01	01	01	01	01	01	01	01	01	01	01	01	01
2	00	00	10	00	11	00	11	00	11	00	11	00	11	00	11	00	11	00	11
3	00	00	11	01	10	01	10	01	10	01	10	01	10	01	10	01	10	01	10
4	00	01	00	00	00	11	11	00	00	11	11	00	00	11	11	00	00	11	11
5	00	01	01	01	01	10	10	01	01	10	10	01	01	10	10	01	01	10	10
6	00	01	10	00	11	11	00	00	11	11	00	00	11	11	00	00	11	11	00
7	00	01	11	01	10	10	01	01	10	10	01	01	10	10	01	01	10	10	01
8	00	10	00	00	00	00	00	11	11	11	11	00	00	00	00	11	11	11	11
9	00	10	01	01	01	01	01	10	10	10	10	01	01	01	01	10	10	10	10
10	00	10	10	00	11	00	11	11	00	11	00	00	11	00	11	11	00	11	00
11	00	10	11	01	10	01	10	10	01	10	01	01	10	01	10	10	01	10	01
12	00	11	00	00	00	11	11	11	11	00	00	00	00	11	11	11	11	00	00
13	00	11	01	01	01	10	10	10	10	01	01	01	01	10	10	10	10	01	01
14	00	11	10	00	11	11	00	11	00	00	11	00	11	11	00	11	00	00	11
15	00	11	11	01	10	10	01	10	01	01	10	01	10	10	01	10	01	01	10
16	01	00	00	00	00	00	00	00	00	00	00	11	11	11	11	11	11	11	11

Table 2 (contd)

Word No.	Data Word			Coded Word															
				t_0 → Time → t_{8i}															
17	01	00	01	01	01	01	01	01	01	01	01	10	10	10	10	10	10	10	10
18	01	00	10	00	11	00	11	00	11	00	11	11	00	11	00	11	00	11	00
19	01	00	11	01	10	01	10	01	10	01	10	10	01	10	01	10	01	10	01
20	01	01	00	00	00	11	11	00	00	11	11	11	11	00	00	11	11	00	00
21	01	01	01	01	01	10	10	01	01	10	10	10	10	01	01	10	10	01	01
22	01	01	10	00	11	11	00	00	11	11	00	11	00	00	11	11	00	00	11
23	01	01	11	01	10	10	01	01	10	10	01	10	01	01	10	10	01	01	10
24	01	10	00	00	00	00	00	11	11	11	11	11	11	11	11	00	00	00	00
25	01	10	01	01	01	01	01	10	10	10	10	10	10	10	10	01	01	01	01
26	01	10	10	00	11	00	11	11	00	11	00	11	00	11	00	00	11	00	11
27	01	10	11	01	10	01	10	10	01	10	01	10	01	10	01	01	10	01	10
28	01	11	00	00	00	11	11	11	11	00	00	11	11	00	00	00	00	11	11
29	01	11	01	01	01	10	10	10	10	01	01	10	10	01	01	01	01	10	10
30	01	11	10	00	11	11	00	11	00	00	11	11	00	00	11	00	11	11	00
31	01	11	11	01	10	10	01	10	01	01	10	10	01	01	10	01	10	10	01
32	10	00	00	10	01	01	10	01	10	10	01	01	10	10	01	10	01	01	10
33	10	00	01	11	00	00	11	00	11	11	00	00	11	11	00	11	00	00	11
34	10	00	10	10	10	01	01	01	01	10	10	01	01	10	10	10	10	01	01
35	10	00	11	11	11	00	00	00	00	11	11	00	00	11	11	11	11	00	00
36	10	01	00	10	01	10	01	01	10	01	10	01	10	01	10	10	01	10	01
37	10	01	01	11	00	11	00	00	11	00	11	00	11	00	11	11	00	11	00
38	10	01	10	10	10	10	10	01	01	01	01	01	01	01	01	01	10	10	10	10
39	10	01	11	11	11	11	11	00	00	00	00	00	00	00	00	00	11	11	11	11
40	10	10	00	10	01	01	10	10	01	01	10	01	10	10	01	01	10	10	01
41	10	10	01	11	00	00	11	11	00	00	11	00	11	11	00	00	11	11	00
42	10	10	10	10	10	01	01	10	10	01	01	01	01	10	10	01	01	10	10
43	10	10	11	11	11	00	00	11	11	00	00	00	00	11	11	00	00	11	11
44	10	11	00	10	01	10	01	10	01	10	01	01	10	01	10	01	10	01	10
45	10	11	01	11	00	11	00	11	00	11	00	00	11	00	11	00	11	00	11
46	10	11	10	10	10	10	10	10	10	10	10	01	01	01	01	01	01	01	01
47	10	11	11	11	11	11	11	11	11	11	11	00	00	00	00	00	00	00	00
48	11	00	00	10	01	01	10	01	10	10	01	10	01	01	10	01	10	10	01
49	11	00	01	11	00	00	11	00	11	11	00	11	00	00	11	00	11	11	00
50	11	00	10	10	10	01	01	01	01	10	10	10	10	01	01	01	01	10	10
51	11	00	11	11	11	00	00	00	00	11	11	11	11	00	00	00	00	11	11
52	11	01	00	10	01	10	01	01	10	01	10	10	01	10	01	01	10	01	10
53	11	01	01	11	00	11	00	00	11	00	11	11	00	11	00	00	11	00	11
54	11	01	10	10	10	10	10	01	01	01	01	10	10	10	10	01	01	01	01
55	11	01	11	11	11	11	11	00	00	00	00	11	11	11	11	00	00	00	00
56	11	10	00	10	01	01	10	10	01	01	10	10	01	01	10	10	01	01	10
57	11	10	01	11	00	00	11	11	00	00	11	11	00	00	11	11	00	00	11
58	11	10	10	10	10	01	01	10	10	01	01	10	10	01	01	10	10	01	01
59	11	10	11	11	11	00	00	11	11	00	00	11	11	00	00	11	11	00	00
60	11	11	00	10	01	10	01	10	01	10	01	10	01	10	01	10	01	10	01
61	11	11	01	11	00	11	00	11	00	11	00	11	00	11	00	11	00	11	00
62	11	11	10	10	10	10	10	10	10	10	10	10	10	10	10	10	10	10	10
63	11	11	11	11	11	11	11	11	11	11	11	11	11	11	11	11	11	11	11

Because the subcarrier is biphase-modulated, it is necessary first to provide an estimate of the data to obtain a signal for the loop to track. This is provided by the filter and limiter acting on the signal in the data channel.

An inlock signal is obtained by demodulating the signal with a subcarrier shifted 90 deg and by comparing the amplitude so obtained with that likewise obtained from the data channel. When the subcarrier loop is in lock, the waveform in the data channel contains components due to the signal as well as noise, but that in the quadrature channel contains only noise. The two channels are constrained to have the same gain and bandwidth so that the noise components are equal and are rejected by the difference amplifier. When the subcarrier loop is out of lock, the phase of the voltage-controlled oscillator is unrelated to the phase of the subcarrier, so the outputs of both the data channel and quadrature channel are the same, and the difference amplifier output is zero.

The data waveform is integrated symbol by symbol, and the individual symbol integrals are passed to the cross-correlator and symbol-timing assembly, where they are combined 32 at a time to produce a true maximum-likelihood detection of the encoded data.

2. Cross-correlator and symbol-timing. For wide-range applicability, this digital equipment is designed to receive symbols at rates as high as 200,000 symbols/s, although the initial requirement for *Mariner* Mars 1969 is only 86,400 symbols/s. The equipment may be controlled by the system computer to process code words whose symbol length is either 16, 32, or 64. The basic part of the assembly receives consecutive code words of

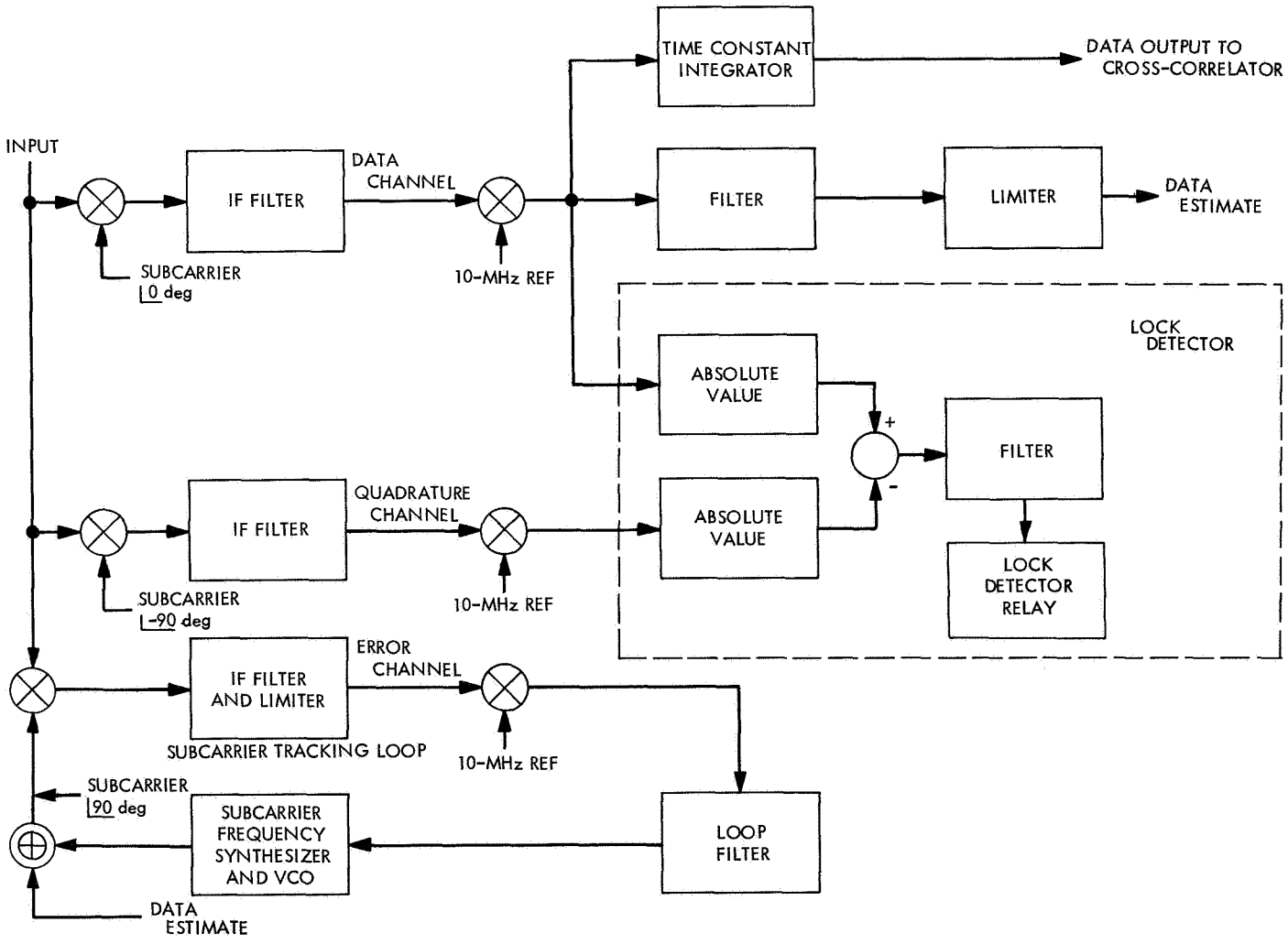

Fig. 11. Subcarrier demodulation assembly

information, and cross-correlates each received word with all code words of the code dictionary. Information bits of the dictionary word with the highest correlation value are packed into a 24-bit register. (This is another reason for using a 6-bit word.) A second register accumulates this highest correlation value, and a third register accumulates a typical nonhighest correlation value. Information in these last two registers enables the computer to determine the SNR of the received telemetry signal. After processing a number of words, the cross-correlation detector transfers the register information to the system computer, the registers are reset to zero, and the process is repeated for the next batch of code words. The number of words processed before information is given to the computer depends upon the computer word length, which is 24 bits. Thus, for *Mariner* Mars 1969, which uses a 6-bit code word, four words will be accumulated for each read-in operation.

Figure 12 is a block diagram of the assembly showing the cross-correlator and the symbol and word-acquisition loops. The partially integrated signal that was the SDA output goes to the symbol-timing loop, and also goes to the cross-correlation detector. Sampling of the signal is performed by analog-to-digital converters (A/DC) under control of the symbol-sync pulses from the symbol-timing loop. The comma-free code vector is removed, and the signal code is cross-correlated with half of the code dictionary. A high positive correlation value indicates the most probably correct dictionary word. A high negative correlation value indicates that the *ones'* complement of the selected dictionary word is the most probable. The results of the correlation go to a comparator, which puts the largest correlation value into the "largest" accumulator, the corresponding information bits into the decoder accumulator, and a typical nonlargest correlation value into the "nonlargest" accumulator. This nonlargest value is usually equal to the correlation between the code word and the last word in the code dictionary. However, if the last correlation value is the largest, then the nonlargest value is set to zero. Compensation for the zeros is made in the algorithm for the estimate of noise. After the required number of words have been processed, the information is transferred to the system computer via the computer interface.

The ratio of the largest correlation value to the typical correlation value is used in synchronizing the symbol counter to the incoming signal. This ratio should be much greater for the in-phase condition than for any of the out-of-phase conditions because of the comma-free character of the code. Accordingly, in the word-acquisition mode, the computer periodically shifts the symbol counter. After each shift, the computer calculates and records the SNR. All possible phases will have been examined when the number of shifts equals the number of symbols in a code word. After examining its table of ratios, the computer again shifts the word origin to that phase having the highest ratio.

To facilitate equipment design, two unusual system concepts have been used. The first of these is a digital integrate-and-dump, forming the basic quantities to be processed by the remaining system. Normally, at low data rates, this function is accomplished by an analog circuit that th n feeds an A/DC for the remaining digital processing. At ..gh data rates, the disadvantages of the dump inaccuracy and lost time could be avoided by replacing the integrate-and-dump circuit with a perfect integrator, digitally subtracting the previous output of the A/DC from the present output to obtain the desired integral over the past period. Exact implementation of this scheme is not feasible for two reasons. First, noise and drift might saturate the integrator; second, calculations show that the effect of the finite levels of quantization in the A/DC can cause high system degradation at low SNR. Therefore, the input to the digital equipment is the output of an imperfect integrator, a simple lowpass RC filter.

After A/D conversion, the digital dump logic calculates an approximation to the required integral ΔE by the equation

$$\Delta E = E_n - \alpha E_{n-1}$$

where E_n is the present voltage sample, E_{n-1} is the previous voltage sample, and α is a positive constant less than unity. The constant α, the filter time constant RC, and the sample or symbol period T are interrelated as follows: assuming a step input voltage E to the filter, the output changes by

$$\Delta E = E(1 - e^{-T/RC}) + E_{n-1}(e^{-T/RC} - \alpha)$$

To eliminate the dependence of ΔE on E_{n-1}, α is chosen to be equal to $e^{-T/RC}$ and for ease in digital implementation, α is made to be equal to $1 - 2^{-N}$ where N is a positive integer.

This imperfect integration of the symbols causes some degradation of system efficiency, depending on the design ST_B/N_0, the number of A/D quantization levels, and the A/D maximum voltage swing. Assuming that the range of the D/AC is ± 3 times the rms value of the input signal plus noise, a value of $N = 3$ is used because the corresponding value of $T/RC = 0.134$ gives least degradation for 7- and 8-bit conversion and negligible

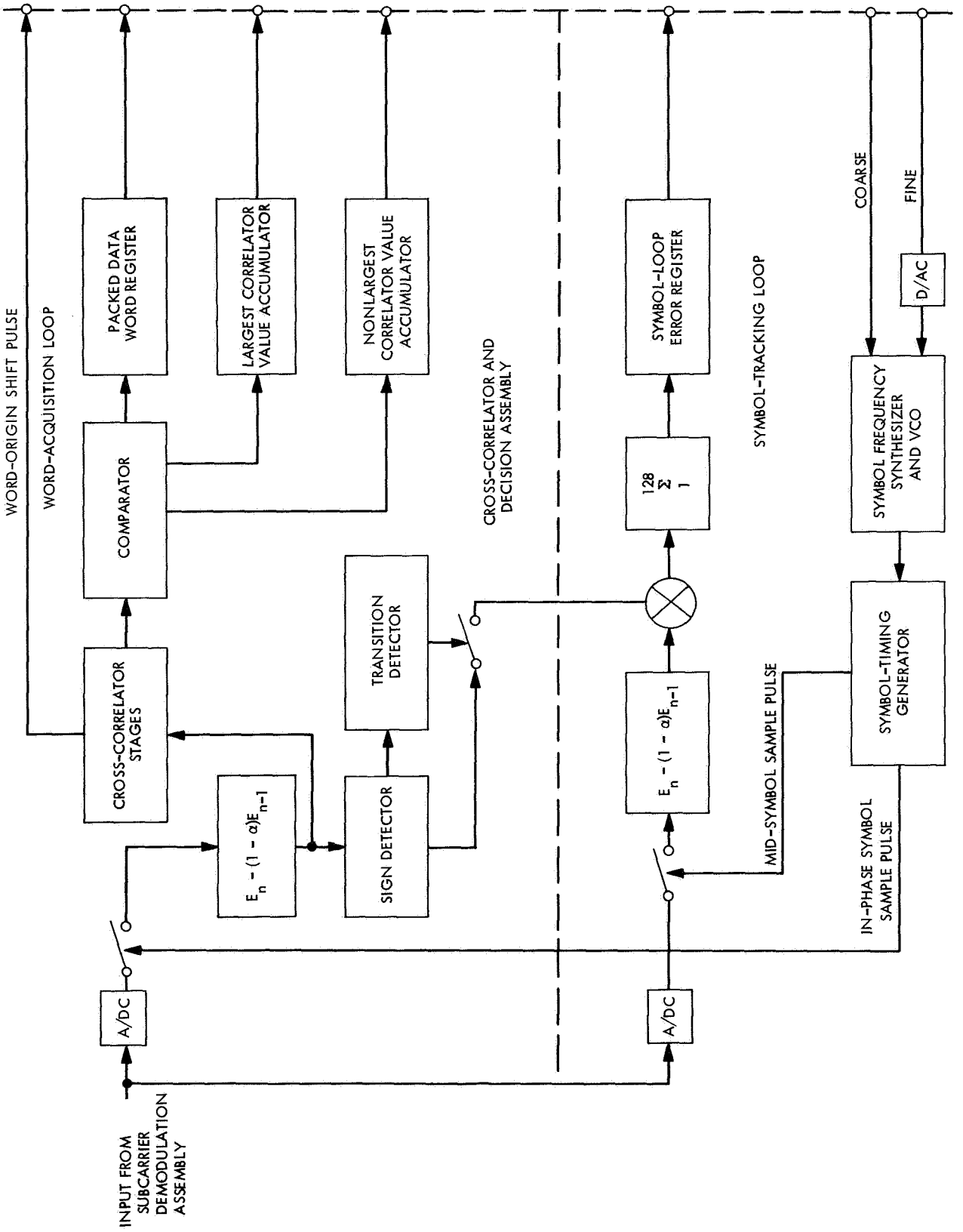

Fig. 12. Cross-correlator and symbol-timing assembly

degradation for higher bit conversions. For the *Mariner* Mars 1969 mission, the symbol period for a symbol rate of 86,400 symbols/s is 11.574 μs. The required value for the SDA integrator time-constant is then 86.4 μs.

Timing for both the symbol integrator and the cross-correlator is provided by a symbol-tracking loop that tracks transitions in the data waveform. Essentially, the loop operates to maintain a zero value for the integrals of the data waveform from the center of one symbol period to the center of the following one, whenever a transition occurs. The occurrence of a transition and its direction are detected by a comparison of the signs of the integrals over the two symbol periods. Thus, if the midsymbol timing tends to drift away from the center of the symbol period, an error signal is generated to correct the midsymbol timing. Since the symbol timing is derived from the midsymbol timing, symbol timing is also corrected and made to coincide with the symbol transitions in the data waveform.

The second unusual system concept used by the digital equipment is the method of correlation. Correlation of the incoming signal code word with a particular dictionary word consists of the multiplication of each symbol integral by its corresponding dictionary word symbol. These products are then summed to give the correlation value. Because the dictionary word symbols are assigned values of either $+1$ or -1, the correlation process reduces to one of simple addition or subtraction of the signal integrals in accordance with the rules of the dictionary code word. The codes capable of being detected by the digital equipment are Reed–Muller biorthogonal (q,n) binary codes that have 2^n dictionary words and q symbols, with $q = 2^{n-1}$. A biorthogonal code dictionary may have its words divided into two groups, a word in one group being the complement of a word in the second group; therefore, a signal word need only be correlated with the 2^{n-1} orthogonal words in one group. A large negative correlation value would then indicate that the dictionary word corresponding to the signal word is to be complemented.

The detection equipment makes use of a special hierarchical structure of the Reed–Muller dictionary. To illustrate the method, consider first the (2,2) code

$$(0) \rightarrow (+1, +1)$$
$$(1) \rightarrow (+1, -1)$$

The maximum-likelihood technique imposes certain rules for forming the correlation values from the sequentially incoming symbol integrals Y_n; for the simple (2,2) code above, these are $(Y_0 + Y_1)$ for dictionary word 0, and $(Y_0 - Y_1)$ for dictionary word 1. Similarly, the word that follows has correlation values $(Y_2 + Y_3)$, etc.

Figure 13 is a block diagram of equipment to obtain the (2,2) code correlations. The input is serialized values of the Ys obtained from the digital dump described above. Starting with the switch in position 1, the serial value of Y_0 enters and fills the shift register. The switch is then placed in position 2, and Y_0 comes out of the register while Y_1 appears on the input line. The adder output $Y_0 + Y_1$ goes out of the equipment while the subtractor output Y_0 as Y_0 is coming out. Upon completion of this operation, the switch is returned to position 1, and the value $Y_0 - Y_1$ comes out of the register and out of the equipment. Simultaneously, Y_2 from the next incoming word fills into the shift register directly behind the value of $Y_0 - Y_1$, and the next cycle is begun. There is a one-to-one correspondence between incoming symbol values and outgoing correlation values, with an appropriate delay, as the equipment cannot start calculating correlation values for a particular word until receipt of the last symbol of that word.

The next code in the hierarchy is the (4,3) code

$$\begin{array}{l} (0) \rightarrow (+1, +1 \,|\, +1, +1) \\ (1) \rightarrow (+1, -1 \,|\, +1, -1) \\ \hline (2) \rightarrow (+1, +1 \,|\, -1, -1) \\ (3) \rightarrow (+1, -1 \,|\, -1, +1) \end{array}$$

This code is formed by four groups of the previous (2,2) code. The lower right-hand group is the complement of the (2,2) code, just as the lower right-hand symbol of the (2,2) code is the complement of the other symbols. Incoming symbol integrals have four values, labeled Y_0 through Y_3 for the first word, Y_4 through Y_7 for the next word, etc. Correlation values for two words are formed following the rules of the code as before,

$$(Y_0 + Y_1) + (Y_2 + Y_3)$$
$$(Y_0 - Y_1) + (Y_2 - Y_3)$$
$$(Y_0 + Y_1) - (Y_2 + Y_3)$$
$$(Y_0 - Y_1) - (Y_2 - Y_3)$$

but are shown with a particular grouping. It should be noted that the correlation values of the (4,3) code are formed by operating on values that can be obtained

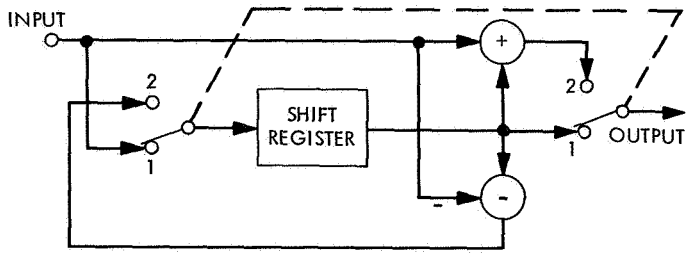

Fig. 13. Simple correlation stage for (2,2) biorthogonal code

pairwise from the equipment shown in Fig. 13, and these values themselves are to be manipulated in exactly the same way, once the two sums and differences have been computed. Equipment for calculating (4,3) code correlation values is thus formed by cascading two stages of equipment, each stage being equivalent to that shown. The first stage operates as described for the (2,2) code. The second stage has a shift register twice as long as the previous stage, and the switch dwells at each switch position for two symbol times.

The (8,4) code is constructed from the (4,3) code in the same way that the (4,3) code was constructed from the (2,2) code. Detection is mechanized by cascading a third stage to the previous two stages where the register length is twice as long as that in the preceding stage, and the switch dwell time is again twice as long. The technique extends readily: the (16,5) code uses four stages, the (32,6) code uses five stages, and the (64,7) code requires six stages. The digital equipment can thus detect words for any code in the hierarchy merely by selecting the output of the proper stage.

3. The software package. Control of synchronization and maintenance of timing accuracy are accomplished under computer control. The computer also functions, as mentioned previously, to format the detected data, along with lock and system-diagnostic information, and to record these data for the user.

It is characteristic of real-time programs that not all functions are required in each mode of operation. For example, a different set of functions is performed during acquisition than is performed in a tracking mode. The software block diagram (Fig. 14) indicates the various functions that are performed in the different sequential modes. There are four such modes, labeled 0 through 3; these are, respectively, an initialization mode, a symbol-acquisition mode, a word-acquisition mode, and finally a data mode. A transition between two modes of operation occurs in response to a certain set of conditions. It should be clearly understood that the program can be in only one of the four modes at any particular time. Furthermore, under normal operating conditions, the program (following loading) progresses sequentially through modes 0, 1, and 2 until mode 3 is reached, in which mode the program remains until data reception is terminated. Mode 0 (initialization) is not indicated on the diagram, as its sole function is to configure the software properly for modes 1, 2, and 3, and to check the system configuration (e.g., tape units ready).

The software diagram displays the overall function of the program and is properly a part of the system block diagram. To turn the functional requirement into an operating unit, however, there must be a technique analogous to that used to turn hardware functions into hardware. For software, this technique consists of a hierarchy of documentation, the first of which is the functional block diagram.

The second level of drawings consists of a sequencing chart for each mode. A sequencing chart has somewhat the same form as a conventional flow chart, but it is concerned with the manner in which the several functions required in a given mode are called up when required. The functions are shown only as blocks, and the chart shows the queueing scheme, the links to other modes, and the operation of interrupts. In cases where timing is critical, the chart is replaced by a timing diagram.

The next level of drawings consists of a detailed flow chart for each of the functions to be performed in each mode. The machine program is derived from these flow charts, and represents the final level of documentation.

The program itself operates as a slave to priority interrupts from the cross-correlator. Some of the functions, such as operator messages and data recording, can be somewhat asynchronous to their data inputs, although they are directly tied to them. Other functions, such as the data inputs themselves, must be performed at once, interrupting any asynchronous processing that the computer might be performing. Data interrupts are generated by the special-purpose digital equipment and occur at the rate of one for each four channel word times.

Some of the functions performed by data-interrupt routines are, e.g., (1) input packed data word and store, (2) input maximum correlation value μ and accumulate single precision, (3) input nonmaximum correlation value σ and accumulate single precision, (4) input symbol data and update symbol-tracking loop, (5) check carrier-loop

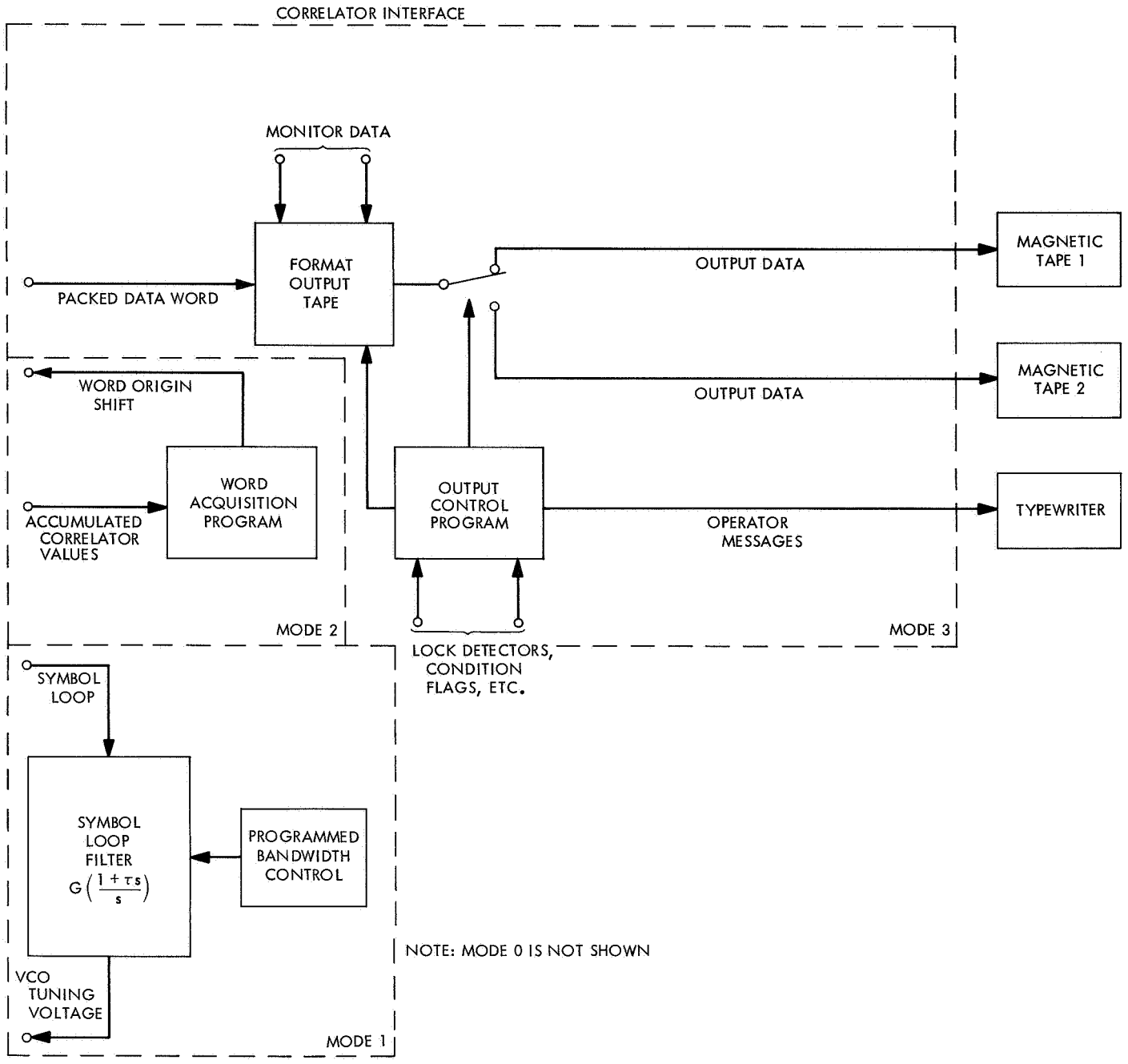

Fig. 14. Software functional diagram

lock status, (6) check subcarrier-loop lock status, (7) check symbol-loop lock status, and (8) augment μ and σ double precision accumulations.

The data words are input in groups of 4 6-bit words and written on tape in groups of 4096 6-bit words (1024 24-bit words), each group comprising one record on magnetic tape. Two tables are reserved in memory, each of which is the length of one record on magnetic tape. During data recording, the program is simultaneously filling one table while the other is being emptied onto magnetic tape. The magnetic tape recording rate is approximately five times the data input rate, so that recording of one table is completed well ahead of a table-full indication for the other table. When a table-full indication occurs, the program immediately switches over and begins to store data in the empty table, while simultaneously initiating recording of the table just filled.

V. System Verification

Once the system was functionally designed and analyzed, there remained not only the construction phase, but also the development of equipment and techniques to verify the design. The primary objective was, of course, to provide an operative flight/ground system having the desired characteristic, with a constraint that the prototype ground system be sufficiently operational upon delivery of the flight equipment to be used as operational support for the spacecraft test. Thus, from the very first, the HRT project entered into design verification studies in parallel with design, analysis, and equipment construction. By the time Lab Set A was delivered for its checkout, a method had been devised to qualify the entire ground telemetry function or any of its parts in a relatively short time, and with excellent accuracy.

A. System Design Verification

Testing of the low-speed breadboard and Lab Set A had at its disposal a specially built receiver–exciter system simulator in which signal and noise parameters could be adjusted and measured with accuracy better than 0.1 dB. As a second check, and for consistency in estimating the parameters, the system computer was programmed to sample the input stream and to compute the same signal and noise values in an independent way. For further flexibility, the SDS-920 computer normally in the tracking stations was replaced in the verification laboratory with an SDS-930 (five times the speed) so that special hardware and software checkout, monitoring, and data reduction could be done easily in real time. This made it possible to perform intense, accurate, detail testing of both the techniques and the hardware.

B. Ground System Integration

At the end of the design-verification phase, Lab Set A was moved to CTA-21, which is the functional extraction of a tracking station. There the lab set was installed in the same way, and mated to equipment identical to equipment that it would encounter later. It was necessary, at this time, to have a way of verifying the high-rate function in order to qualify the ground station as ready and able to support simulated operations with a spacecraft located in the assembly facility, the space simulator, or the environmental test area. To this end, a piece of test equipment had simultaneously been constructed. The HRT system test equipment provides test signals that are electrically equivalent to those of the received telemetry data stream, and that can be sent to any of several inputs of the HRT subsystem for performing checks. Generation of the code and its modulation onto a subcarrier are similar to those functions in the spacecraft. The data source, however, is different.

The information words to be transmitted are generated by a 9-stage modified pseudonoise shift-register generator, which provides a series of states in a sequence that repeats every 512 word times. Each 6-bit word appears pseudorandomly eight times during every 512-word sequence. Being thus generated by a shift register, the data words have five of their six bits identical, except for a one-bit shift. This latter property makes it possible to detect errors introduced into the system merely by comparing adjacent words recorded on the output magnetic tape.

To exercise the entire HRT function, a test signal is introduced at the S-band carrier frequency, and errors are counted from the output tape record. The word-error rate of the demodulated telemetry and the reliability of correct word acquisition as functions of the RF input SNR can thus be measured as the desired verification of performance.

The sideband modulation index of the S-band test signal is first adjusted for a specific sideband-to-carrier ratio, viz, the same value it will have during actual spacecraft operation. Then, without modulation, the carrier-to-noise ratio (CNR) is set to give the required sideband-to-noise energy ratio when modulation is applied. Next, modulation is applied, and the performance of the HRT function is judged by the word-error-rate ratios having expected data-word-error rates of roughly 0.1, 1, and 23.3%. The latter figure is a 10% bit-error probability. Finally, the reliability of correct word acquisition is tested at the sideband-to-noise ratio having an expected word-error rate of 23.3%.

Figure 15 is a block diagram of the SNR configuration. The HRT test-set data modulates a test translator or transmitter; the resulting S-band test signal is applied to the receiver and detected as if the spacecraft were the actual source. The S-band input SNR is established at the receiver input by monitoring the heterodyne signal at 50 MHz, using the special SNR measurement assembly shown.

The technique used consists of measuring the ratio of carrier-plus-noise power to noise power very accurately. First, the power indicator (M1 in the figure) is adjusted for full-scale deflection with the RF signal source off (noise only). Then the desired SNR, taking into account

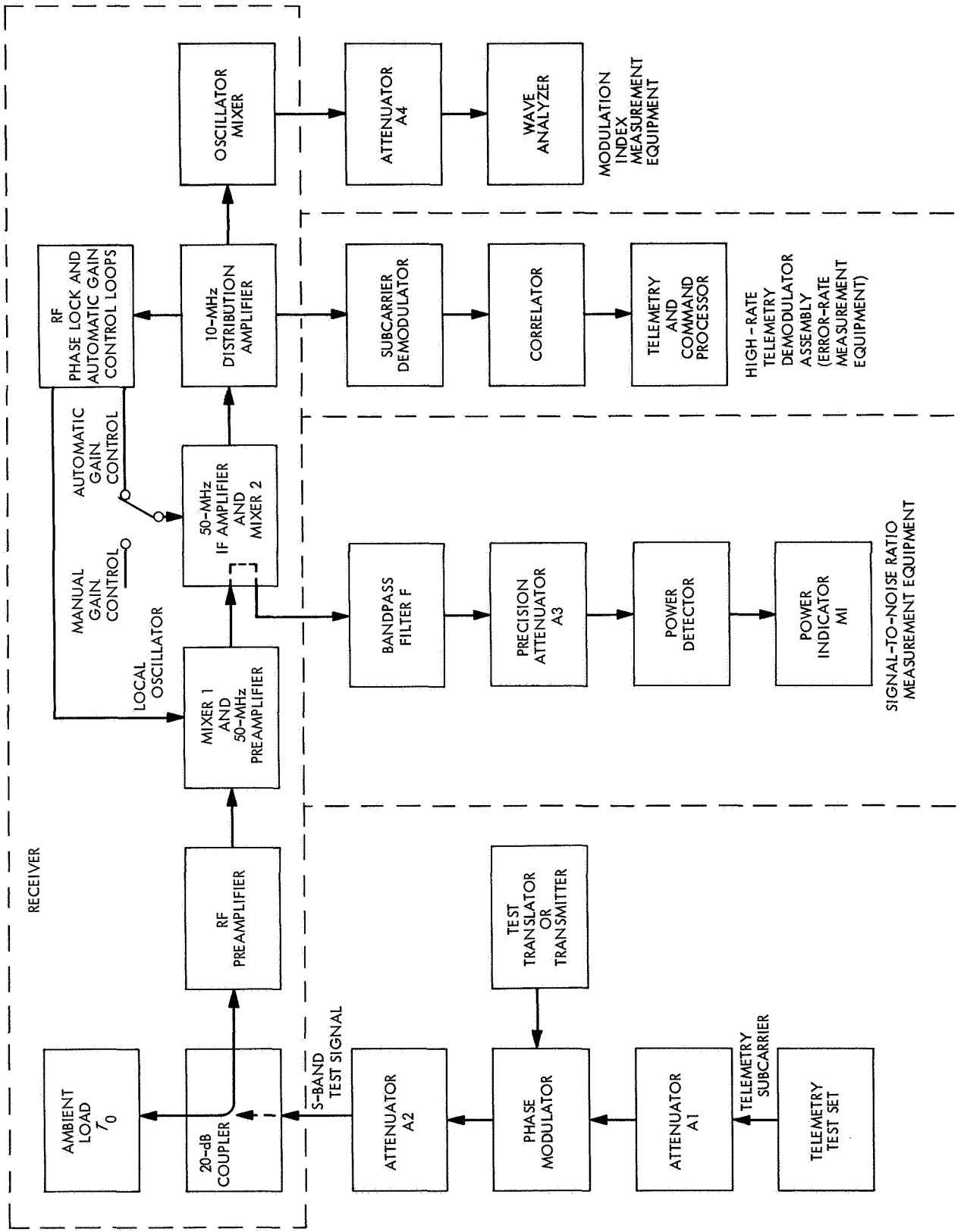

Fig. 15. Configuration for accurate measurement of ST_B/N_0

the bandwidth of filter F, is inserted in the precision attenuator A3, and, with the unmodulated signal source turned on, A2 is adjusted until the power level at M1 is returned to the same value.

The accuracy of measuring a given CNR is determined solely by attenuator A3 and bandpass filter F, assuming a stable signal level and white noise. The accuracy with which the bandwidth of F is known is given as ±0.01 dB. The accuracy of the precision attenuator is given by the manufacturer as ±0.1 dB for the worst case. Thus, the accuracy in $(P_c + N)/N$ is ±0.11 (or 2.5%) dB for the worst case.

The accuracy also depends on how precisely the modulation index can be set. The carrier-suppression method, modified slightly, proves to be very accurate. With the receiver locked to the incoming carrier at a strong signal, a convenient level is set on a wave analyzer. Attenuation equal to the desired carrier suppression is inserted in a precision attenuator, and a reference level measured on the meter. The attenuator is then returned to its original setting, and modulation is applied until the reference level is again reached. The accuracy is solely a function of the quality of the precision attenuator, which is published to be 0.1 dB by the manufacturer. At the suppression used, this reflects only about 0.02 dB change in sideband power, however. The total accuracy of the method is thus about 0.13 dB at large ST_B/N_0 to about 0.2 dB at a bit-error rate of 10%. [An error of 0.11 dB in $(P_c + N)/N$ can cause about 0.18 dB error in P_c/N_0 at $ST_B/N_0 = 0.817$, corresponding to a 10% bit-error rate.]

C. Flight/Ground System Verification Tests

Following the installation and verification of the high-rate ground equipment described above, the *Mariner* Mars 1969 project telecommunications system group began initial testing of the high-rate channel, using spacecraft breadboard telemetry and radio equipment. At the time of this report, the spacecraft breadboard equipment had been completely tested, and initial testing had begun on the first spacecraft (the proof-test model). The data source for the breadboard test consisted of a simulator that generated all *ones, zeros,* or a pseudorandom sequence of uncoded data words for the input to the telemetry breadboard block encoder. The block-coded output (the coded words), phase-modulated onto the 259.2-kHz subcarrier, was sent through an attenuator to the spacecraft breadboard radio modulator–transmitter. The RF signal from the spacecraft was passed through a hard-line RF path to the compatibility-test ground receiver. The same technique described earlier for obtaining precisely measured values of ST_B/N_0 for ground-system verification was also used for spacecraft testing.

The finite rise and fall times and the asymmetry of the waveform cause an equivalent signal loss of approximately 0.5 dB (12%). Approximately 0.23 dB (5.5%) of this value can theoretically be attributed to the subcarrier waveform asymmetry. This was verified by comparing the performance of the spacecraft breadboard with a laboratory reference waveform having extremely steep rise and fall times and no discernible asymmetry. Care is thus being taken to shape the flight spacecraft waveforms to limit this loss to less than 0.2 dB. The loss component due to rise and fall times was automatically compensated for in this test by adjusting the power allocations for each channel.

The performance measurement in this test was a word-error measurement, the results of which are shown in Fig. 16 for various values of ST_B/N_0. The test data indicate a 1% error rate for $ST_B/N_0 = 3.9$ dB, compared to a theoretical 100% efficient value of 3.0 dB. The 0.9-dB difference is the measured efficiency of the system hardware. Almost all of this difference can be attributed to calculated design efficiencies of the various components in the system:

Waveform asymmetry	= 0.2 dB (5%)	= 0.8 dB (20%)
Ground system (Rcvr, SDA, CC, etc.)	= 0.4 dB (10%)	
SNR measurement	= 0.2 dB (5%)	

leaving only 0.1 dB unaccounted for in the theory.

VI. Conclusion

This report has given some of the rationale and design philosophy that have produced the *Mariner* Mars 1969 HRT system. All of the detailed analyses and many of the special hardware-implementation techniques have been omitted in consideration of space limitations. The interested reader, however, can find these in the references cited.

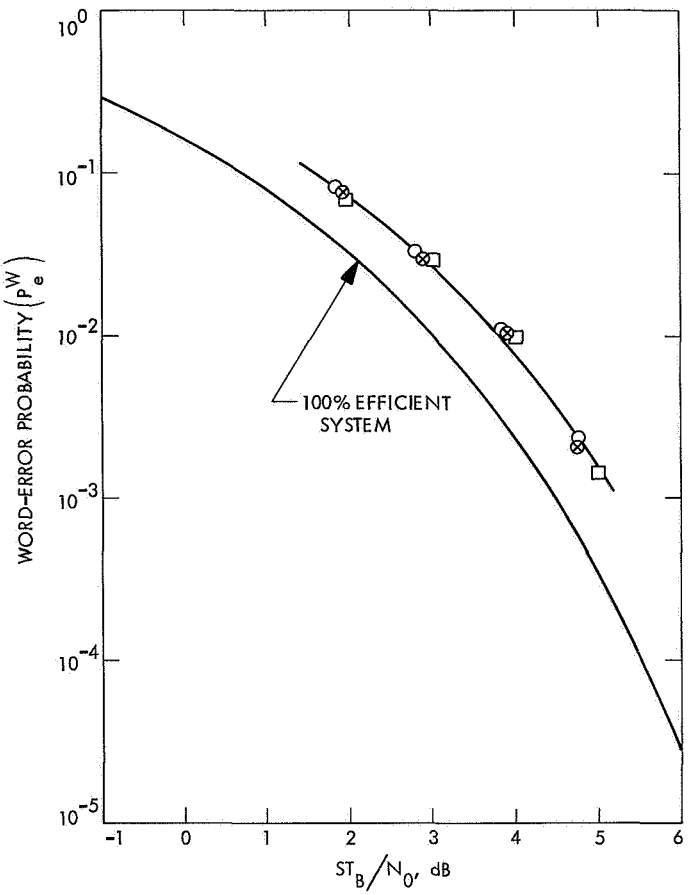

Fig. 16. Measured and 100% efficient performance curves for the HRT system

References

1. Easterling, M., et al., "High-Rate Telemetry Project," in *The Deep Space Network,* Space Programs Summary 37-48, Vol. II, pp. 83–130. Jet Propulsion Laboratory, Pasadena, Calif., Nov. 30, 1967.

2. Tausworthe, R., et al., "High-Rate Telemetry Project," in *The Deep Space Network,* Space Programs Summary 37-49, Vol. II, pp. 115–127. Jet Propulsion Laboratory, Pasadena, Calif., Jan. 31, 1968.

3. Lindsey, W. C., "Design of Block-Coded Communication Systems," *IEEE Trans. Commun. Technol.,* Vol. COM-15, No. 4, pp. 525–534, Aug. 1967.

4. Golomb, S. W., et al., *Digital Communications With Space Applications,* Chaps. 7 and 8. Prentice-Hall Publishing Co., New York, 1964.